Optical Materials 62 (2016) 7–11

Contents lists available at ScienceDirect

Optical Materials

journal homepage: www.elsevier.com/locate/optmat

Structure, spectroscopic properties and laser performance of Nd:$YNbO_4$ at 1066 nm

Shoujun Ding [a, b], Fang Peng [a], Qingli Zhang [a, *], Jianqiao Luo [a], Wenpeng Liu [a], Dunlu Sun [a], Renqin Dou [a, b], Guihua Sun [a]

[a] Anhui Institute of Optics and Fine Mechanics, Chinese Academy of Sciences, Anhui Province, Hefei 230031, PR China
[b] University of Science and Technology of China, Hefei 230026, PR China

ARTICLE INFO

Article history:
Received 19 July 2016
Received in revised form
15 August 2016
Accepted 12 September 2016
Available online 23 September 2016

Keywords:
Nd:$YNbO_4$
Structure
Spectroscopic properties
Laser performance

ABSTRACT

We have demonstrated continuous wave (CW) laser operation of Nd:$YNbO_4$ crystal at 1066 nm for the first time. A maximum output power of 1.12 W with the incident power of 5.0 W is successfully achieved corresponding to an optical-to-optical conversion efficiency of 22.4% and a slope efficiency of 24.0%. The large absorption cross section (8.7×10^{-20} cm^2) and wide absorption band (6 nm) at around 808 nm indicates the good pumping efficiency by laser diodes (LD). The small emission cross section (29×10^{-20} cm^2) and relative long lifetime of the $^4F_{3/2} \rightarrow {}^4I_{11/2}$ transition indicates good energy storage capacity of Nd:$YNbO_4$. Moreover, the raw materials of Nd:$YNbO_4$ are stable, thus, it can grow high-quality and large-size by Czochralski (CZ) method. Therefore the Nd:$YNbO_4$ crystal is a potentially new laser material suitable for LD pumping.

1. Introduction

Neodymium (Nd) doped materials are one kind of the most important 1.06 μm laser gain mediums of diode pumped solid-state lasers, which have been applied in many fields such as medicine, industry, submarine communications, and so on [1–3]. In recent years, many Nd-doped laser crystal have been discovered and studied deeply, including Nd:YAG, Nd:vanadates, Nd:tantalates, and Nd:LYSO. Among these crystals, Nd-doped vanadate family crystals (ReVO4, Re=Y, Gd, Lu) and tantalate crystals exhibit excellent laser performance [4]. Nd:YVO_4 laser have been commercialized for polarizer and low pumping power laser crystal at present [5]. Nd:$GdVO_4$ have also been proved to be an efficient laser material with slope efficiency of 66% [6]. Nd:$GdTaO_4$ was grown by Fang Peng et al. [7] and 1.06 μm laser output was also realized with slope efficiency of 36%. Besides, Yb,Ho:$GdYTaO_4$ [8] and Tm,Ho:$GdYTaO_4$ [9] are suggested to be promising candidates for 2.911 μm laser. As we know, vanadium, niobium and tantalum belongs to VB group in the periodic table of the elements. Since vanadates and tanalates are good laser host materials, the potential of niobates as laser hosts attracts our interest. Considering the inspiring luminescent properties of $YNbO_4$ [10–12], we choose $YNbO_4$ as the laser host material in this work.

$YNbO_4$ has three types of structure [13,14]: M-type with the space group of I2/a, M′-type with the space group of P2/a, and T-type (high temperature tetragonal phase with the scheelite structure). Usually, M′-type forms at a certain temperature (about 1400 °C), while M-type is obtained during cooling from the melt. The difference between M-type and M′-type is that Nb atom and four O atoms form a distorted tetrahedron in M-type whereas Nb atom coordinates with six O atoms form a distorted octahedron in M′-type. In both M-type and M′-type, the site symmetry of Nb^{5+} and Y^{3+} ions are C_2, and the site symmetry of O^{2-} ion is C_1. When Nd is doped into $YNbO_4$, Nd ions occupy Y sites and thus possess C_2 site symmetry. The low symmetry of Nd^{3+} in $YNbO_4$ benefits to relaxing the parity-forbidden rule and improving the photoluminescence efficiency. Furthermore, polarized laser can be easily realized in crystals with low symmetry [7]. In addition, there is no component volatility in Cz growth of Nd:$YNbO_4$ which is more favorable for the large-size and high-quality crystal growth than Nd-doped vanadate crystals [6]. And Nd-doped $YNbO_4$ has a lower melting point than GTO and GYTO, indicating that the growth of Nd:$YNbO_4$ is more energy-saving.

In this work, a Nd:$YNbO_4$ was grown by Cz method. Its structure, absorption spectrum, fluorescence spectrum and fluorescence decay lifetime were investigated. Besides, the CW laser operation of

* Corresponding author.
E-mail address: zql@aiofm.ac.cn (Q. Zhang).

http://dx.doi.org/10.1016/j.optmat.2016.09.032

$Nd:YNbO_4$ at 1.06 μm was realized by LD pumping.

2. Experimental details

A 1 at% $Nd:YNbO_4$ crystal was grown successfully by the Cz method, with an automatic diameter controlled (ADC) growth system. The oxide powders of Nb_2O_5, Y_2O_3 and Nd_2O_3 with 99.999% purity were used as the starting materials. The raw materials were weighed according to the chemical formula $Nd_{0.01}Y_{0.99}NbO_4$. The mixtures were mixed thoroughly and pressed into disks, and then loaded into iridium (Ir) crucible. The Ir crucible is 60 mm in diameter and 45 mm in height. In order to prevent the iridium crucible from oxidization, the furnace was pumped into the vacuum and then filled with nitrogen. An $YNbO_4$ crystal rod was used as a seed. The pulling rate was 0.35–0.5 mm/h and crystal rotation speed was 3.0–10.0 rpm. After growth, the crystal was cooled down to room temperature at a speed of 30–50 °C/h. The wafers along (100), (010), (001) face of $Nd:YNbO_4$ crystals are shown in Fig. 1.

The structure of $Nd:YNbO_4$ crystal was examined by X-ray diffraction (XRD) using a Philips X'pert PRO X-ray powder diffractometer equipped with Cu Kα radiation. A scan step of 0.033° was applied to record the patterns in the 2θ range of 10°–90°. An X'pert Pro MPD diffractometer equipped with a Hybrid Kα1 monochromator was used to collect the X-ray rocking curve. A thin slice sample was cut from shoulder part of the as-grown crystal, and X-ray fluorescence analysis (XRF-1800) was used to measure the concentration of Nd^{3+} ions in the as-grown crystal. The absorption spectra in the range of 320–2000 nm was recorded by a Perkin-Elmer UV-VIS-NIR Lambda-950 spectrophotometer with a resolution of 0.1 nm. A FLSP-920 spectrophotometer (Edinburgh instrument Ltd, UK) was used to measure the photoluminescence spectrum and the fluorescence decay curve with the excitation of an 808 nm LD and a microsecond-lamp, respectively. All the measurements were carried out at room temperature.

A schematic of the laser experimental setup of the diode end-pumped is shown in Fig. 2. The laser medium was an cuboid $Nd:YNbO_4$ crystal with dimensions of 2 mm × 2 mm × 4 mm, in which the two 2 mm × 2 mm faces are along crystallographic *b* direction. Both of the two 2 mm × 2 mm faces were polished carefully. The pumping source was a fiber-coupled LD with a maximum output power of 30 W and the central wavelength at around 808 nm. Through the focusing optics (N.A. = 0.22), the output beam of the diode laser fiber was focused into the laser crystal with a spot radius of 0.2 mm. A simple plano-plano resonator was used to generate laser. M1 is an input mirror with anti-reflection (AR) coated at 808 nm at the pump side, high-reflection (HR) (99.95%) coated at 1066 nm and high-transmission (HT) coated at 808 nm on the opposite side. M2 is output coupler mirror with two different transmissions (2.6% and 5.4%) at 1066 nm. In order to remove the heat generated by the laser crystal, the crystal was wrapped with indium foil and mounted in a water-cooled copper block. The cooling water temperature was controlled at 18 °C during the whole experiments. The output power was recorded by an OPHIR 30A-BB-18 power meter.

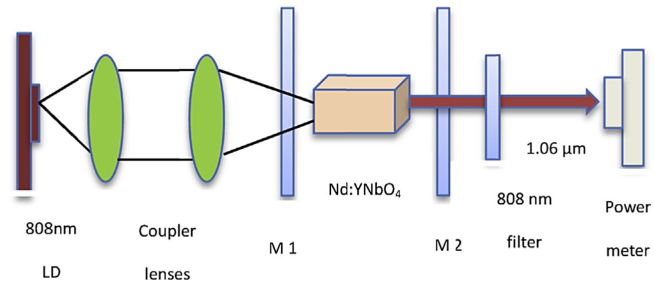

Fig. 2. Schematic of the experimental setup of the diode end-pumped $Nd:YNbO_4$ laser.

3. Results and discussion

3.1. Crystal structure and quality

The XRD pattern of the $Nd:YNbO_4$ crystal is shown in Fig. 3. All the peaks of $Nd:YNbO_4$ crystal can be well indexed with those of ICSD #20335. The as-grown crystal belongs to I2/a space group. Using the general structure analysis software (GSAS) [15], the unit cell parameters of $Nd:YNbO_4$ are obtained to be: a = 7.0409 Å, b = 10.9517 Å, c = 5.3806 Å; $\alpha = \gamma = 90°$, $\beta = 134.07°$. The refined results are shown in Fig. 3. The residual factor *Rp* and weighted residual variance factor *Rwp* are 6.7% and 8.8%, respectively, indicating a reliable refinement result. The X-ray rocking curve of the as-grown crystal along *b* direction is shown in Fig. 4. The full width at half maximum (FWHM) is 0.05°, which indicates a high crystalline quality of the as-grown crystal.

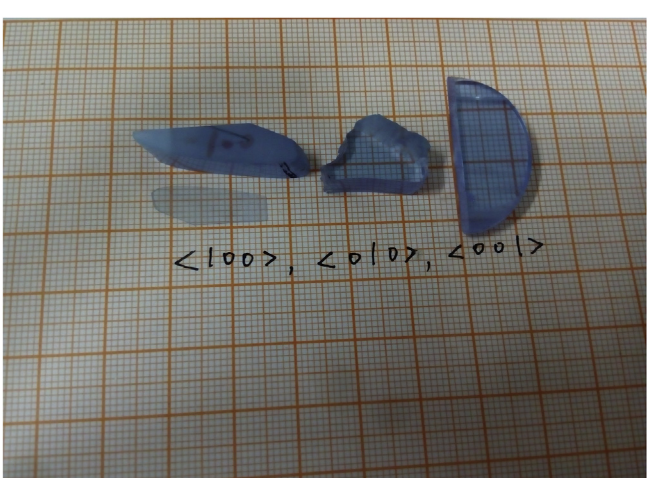

Fig. 1. Photograph of wafers along (100), (010), (001) faces of $Nd:YNbO_4$ crystal.

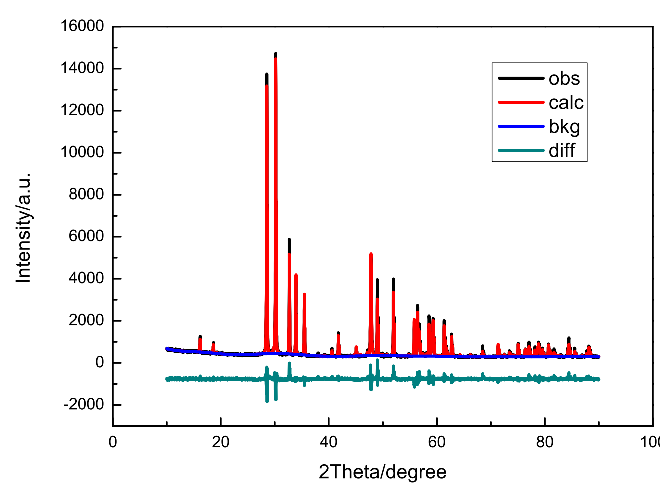

Fig. 3. Rietveld refinement result of $Nd:YNbO_4$ (obs: the observed data; calc: the calculated data; bkg: the background; diff: the difference between observed and calculated data).

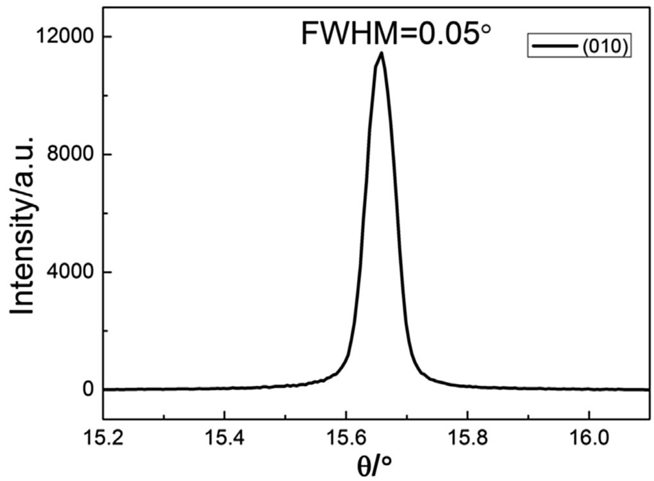

Fig. 4. X-ray rocking curves of as-grown crystal along *b* direction.

3.2. Effective segregation coefficient and refractive index

The segregation coefficient of Nd^{3+} in Nd:$YNbO_4$ crystal was calculated according to the equation $k_{eff} = C_S/C_L$, where C_s and C_L are the respective concentration of the ions in the crystal and the melt. The effective segregation coefficient of Nd^{3+} in $YNbO_4$ is calculated approximately to be 0.5.

Refractive index *n* is an important parameter of crystal, which can be obtained by fitting the absorption spectrum. This method is widely used to measure the refractive index because there is no measurement range restriction and is easy to be operated [16]. The refractive indices can be fitted by the least square method with the following Sellmeier equation [17]. The sample used to calculate the refractive index was cut perpendicularly to the *b* axis.

$$n^2(\lambda) = A + \frac{B}{\lambda^2 - C} + D\lambda^2 \quad (1)$$

The fitted Sellmeier coefficients are A = 3.66287, B = 44887.37 nm^2, C = 2.9531 × 10^6 nm^2, and D = 2.2874 × 10^{-7} nm^{-2}. According to the fitted results, the refractive index at 808 nm is calculated to be 1.95.

3.3. Optical properties

The absorption spectra of Nd:$YNbO_4$ along *a*, *b*, *c* faces are shown in Fig. 5. There are twelve absorption bands corresponding to the characteristic peaks of Nd^{3+} from the ground state $^4I_{9/2}$ to different excited states. All the final states are assigned and denoted in Fig. 5. There is a strong absorption of Nd: $YNbO_4$ crystal at 808 nm which can be well matched with the commercial 808 nm diode laser. Due to the anisotropy of monoclinic system, the absorption coefficients of Nd:$YNbO_4$ at 808 nm along *a*, *b*, *c* axes are 4.11, 5.87, 4.98 cm^{-1}, respectively. The maximum FWHM of Nd:$YNbO_4$ at around 808 nm absorption band is about 6 nm along *b* direction, which is 3 times wider than that of Nd:YAG [7]. The broader absorption band can reduce the dependence of the laser crystal on the temperature control of the pumping source. The absorption cross section σ_α can be calculated by $\sigma_\alpha = \alpha(\lambda)/N$, where α is the absorption coefficient and *N* is the concentration of Nd^{3+} in Nd:$YNbO_4$ crystal. Based on the XRF result, the Nd^{3+} concentration was calculated to be 6.8 × 10^{19} cm^{-3}. Therefore, the maximum absorption cross section of Nd:$YNbO_4$ at 808 nm is calculated to be 8.7 × 10^{-20} cm^2.

The Judd-Ofelt (J-O) theory [18,19], which is widely used to calculate the spectroscopic parameters of rare earth ions doped crystals, is applied to calculate the optical parameters of the electric dipole transition of Nd^{3+} ion in $YNbO_4$ host. The experimental oscillator strength f_{exp}, experimental dipole line strength S_{exp} as well as the calculated electric dipole line strength S_{cal} are listed in Table 1. The relative square deviation *R* is fitted to be 7.3%, indicating a well consistency between the experimental and calculated results.

The three intensity parameters Ω_t (t = 2,4,6) are fitted to be 14.197 × 10^{-20}, 4.303 × 10^{-20} and 6.352 × 10^{-20} cm^2, respectively. Generally, the Ω_2 parameter depends on the structure and symmetry of the crystal. The higher value of Ω_2, the lower local environment symmetry exists [20,21]. The large value of Ω_2 indicates that the low local environment symmetry exists in Nd:$YNbO_4$. The

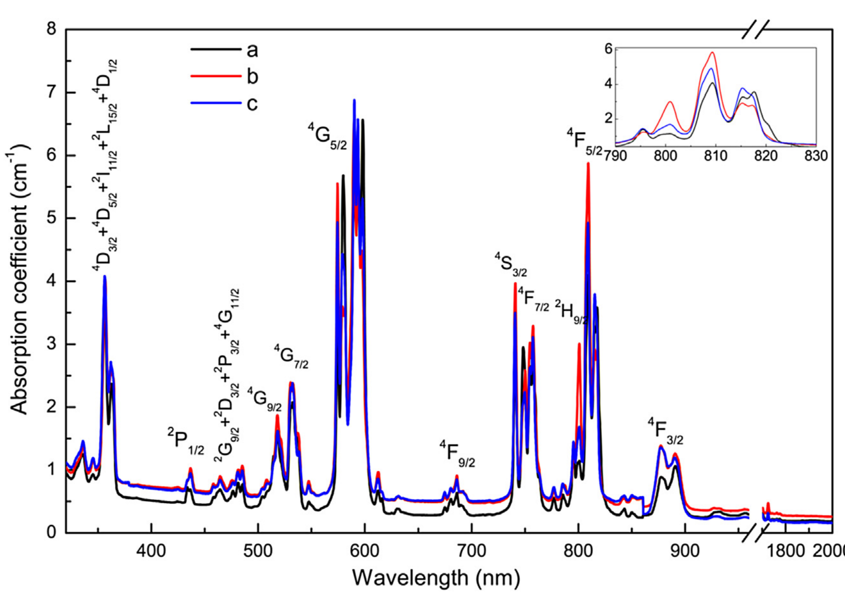

Fig. 5. Absorption spectra of Nd:$YNbO_4$ crystal in three directions at room temperature (the black red and blue lines denote samples in *a*, *b* and *c* directions, respectively). (For interpretation of the references to colour in this figure legend, the reader is referred to the web version of this article.)

Table 1
Spectral parameters of Nd:$YNbO_4$ crystal.

Excited state	$\bar{\lambda}$ (nm)	f_{exp} ($\times 10^{-6}$)	S_{exp} ($\times 10^{-20} cm^2$)	S_{cal} ($\times 10^{-20} cm^2$)
$^4D_{1/2}$+$^4D_{3/2}$+$^4D_{5/2}$+$^2I_{11/2}$+$^2L_{15/2}$	358	13.025	2.343	2.794
$^2P_{1/2}$+$^2D_{5/2}$	433	1.422	0.307	0.184
$^2G_{19/2}$+$^2D_{13/2}$+$^2P_{3/2}$+$^4G_{11/2}$	474	4.971	1.168	0.352
$^4G_{9/2}$+$^2K_{13/2}$	518	4.146	1.065	0.874
$^4G_{7/2}$	535	9.361	2.472	2.017
$^4G_{5/2}$	577	5.203	15.148	15.188
$^4F_{9/2}$	686	1.311	0.444	0.362
$^4S_{3/2}$	739	2.982	1.094	1.488
$^4F_{7/2}$	751	7.543	2.817	2.907
$^2H_{9/2}$	799	2.411	0.954	0.855
$^4F_{5/2}$	808	9.289	3.734	3.545
$^4F_{3/2}$	880	3.974	1.741	1.353
Intensity parameters ($\times 10^{-20}$ cm^2)	$\Omega_2 = 14.197$ $\Omega_4 = 4.303$ $\Omega_6 = 6.352$			

Table 2
Spectral parameters of Nd:$YNbO_4$ for the radiative 4F3/2 → 4IJ′ transition.

Transitions	S_{cal} (10^{-20} cm^2)	$A_{(J''\rightarrow J)}$ (s^{-1})	$\beta_{(J''\rightarrow J')}$ (%)	τ_{rad} (μs)
$^4F_{3/2} \rightarrow {}^4I_{9/2}$	0.911	2008.89	34.39	171.1
$^4F_{3/2} \rightarrow {}^4I_{11/2}$	2.338	3095.51	52.98	
$^4F_{3/2} \rightarrow {}^4I_{13/2}$	1.029	704.16	12.05	
$^4F_{3/2} \rightarrow {}^4I_{15/2}$	0.128	34.28	0.587	

emission properties mainly depends on the values of Ω_4 and Ω_6. In Nd:$YNbO_4$ crystal, the spectroscopic quality parameterΩ_4/Ω_6 is calculated to be 0.68, which is less than 1, indicating that the transition of $^4F_{3/2} \rightarrow {}^4I_{11/2}$ is more efficient than that of $^4F_{3/2} \rightarrow {}^4I_{9/2}$. Based on the obtained J-O intensity parameters, the radiative transition rate A(J″→J′), fluorescence branching ratio β(J″→J′), radiative lifetime can be calculated, which are listed in Table 2. The branching ratio of $^4F_{3/2} \rightarrow {}^4I_{11/2}$ transition is larger than that of $^4F_{3/2} \rightarrow {}^4I_{9/2}$ transition, which demonstrates that Nd:$YNbO_4$ is more suitable to generate 1.06 μm laser.

As listed in Table 2, the radiative lifetime of $^4F_{3/2}$ was calculated to be 171.1 μs. The fluorescence decay curve of the transition of $^4F_{3/2} \rightarrow {}^4I_{11/2}$ excited by 808 nm is shown in Fig. 6. The decay curve can be well fitted with single exponential decay function and the fluorescence lifetime of Nd:$YNbO_4$ was fitted to be 152 μs, which is longer than that of Nd:YVO_4 [22]. Besides, the radiative quantum efficiency of the $^4F_{3/2}$ state is determined to be $\eta = 152/171.1 = 88.83\%$. The results indicate Nd:$YNbO_4$ is a promising laser crystal for 1.06 μm laser.

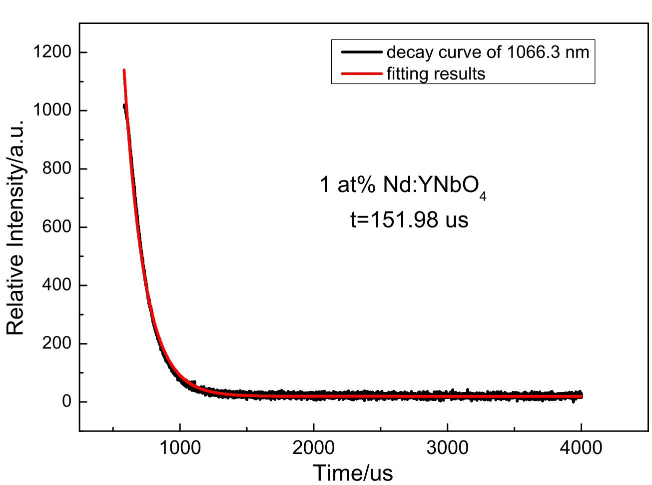

Fig. 6. Fluorescence decay curves of the 4F3/2 → 4I11/2 transition of Nd:$YNbO_4$.

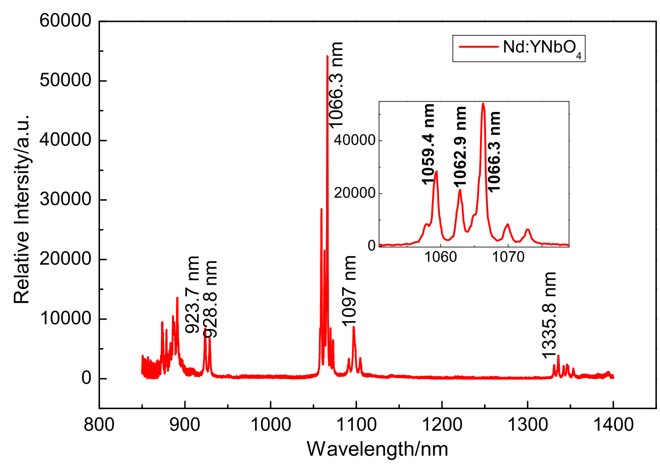

Fig. 7. Emission spectrum of Nd:$YNbO_4$ crystal under 808 nm LD excitation.

The photoluminescence spectrum of Nd:$YNbO_4$ crystal excited by 808 nm LD is shown in Fig. 7. In the range of 850 nm–1400 nm, the strongest emission peak is located at 1066.3 nm, corresponding to the transition of $^4F_{3/2} \rightarrow {}^4I_{11/2}$ of Nd^{3+} ion. The stimulated emission cross section σ_{em} can be calculated from the measured fluorescence spectrum by the Füchtbauer-Ladenburg (F-L) formula [23].

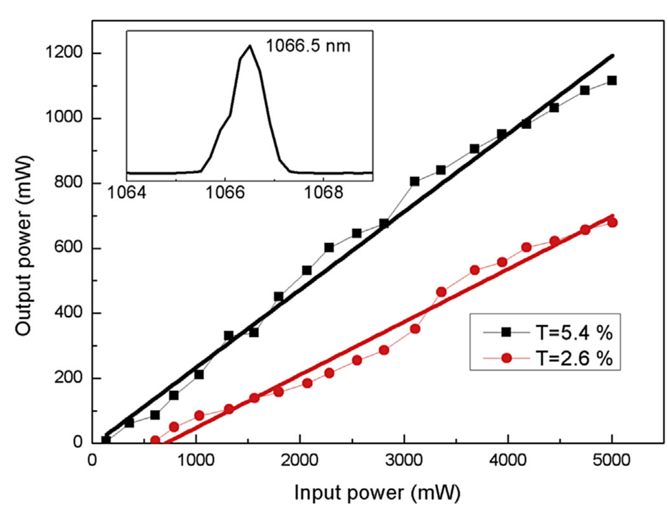

Fig. 8. CW output power of Nd: YNbO4 versus incident power with different output couplers. Insert: the laser spectra of Nd: YNbO4.

Table 3
Comparison of the spectroscopic properties and laser performance of Nd:$YNbO_4$ with other Nd-doped monoclinic laser crystals.

Crystals	η(%) (slope efficiency)	σ_α ($10^{-20}cm^2$)	σ_{em} ($10^{-20}cm^2$)	τ_{em} (μs)	Ref.
Nd:$YNbO_4$	24	8.7	29	152	This work
Nd:LYSO	29	6.1	7.7	226	[20]
Nd:GTO	36	5.1	39	178	[7]
Nd:$LaVO_4$	41	1.7	6.5	193	[24,25]
Nd:KGW	66	23	38	99	[26]

$$\sigma_{em}(\lambda) = \frac{\lambda^5 \cdot I(\lambda)}{8\pi n^2 c \tau_m \int \lambda I(\lambda) d\lambda} \tag{2}$$

where $I(\lambda)$ is the fluorescence intensity, τ_m is the measured lifetime, c is the velocity of light, λ is the emission wavelength, and n is the refractive index. The stimulated emission cross section of Nd:$YNbO_4$ crystal at 1066.3 nm for $^4F_{3/2} \rightarrow {}^4I_{11/2}$ transition was calculated to be 29×10^{-20} cm^2,which is smaller than that of Nd:YVO_4 crystal. The small σ_{em} and long fluorescence lifetime indicates good energy storage capacity of Nd:$YNbO_4$, which is beneficial to its application in Q-switched laser.

3.4. Laser performance

Fig. 8 shows the dependence of output power on the incident pump power with two different output couplers. When the output coupler transmission is 5.4%, a maximum output power of 1.12 W is obtained with an incident pump power of 5.0 W, corresponding to an optical-to-optical conversion efficiency of 22.4% and a slope efficiency of 24.0%, which is better than the output coupler transmission of 2.6%. The threshold powers were measured to be 0.14 W with the output coupler transmission of 5.4%. The comparison of spectroscopic properties and laser performance between Nd:$YNbO_4$ and Nd-doped monoclinic laser crystals is shown in Table 3. It can be concluded that Nd:$YNbO_4$ crystal exhibits good comprehensive spectroscopic performance. The laser performance of Nd:$YNbO_4$ is hopeful to be improved if anti-reflection are coated on both end faces of the crystal and the Nd^{3+} ion concentration is optimized.

4. Conclusions

In conclusion, the growth, spectroscopic, and 1066 nm laser performance of Nd:$YNbO_4$ are reported for the first time, to the best of our knowledge. The effective segregation coefficient of Nd^{3+} ion in $YNbO_4$ is measured to be 0.5. The cell parameters are obtained by Rietveld refinement method. The spectral parameters are calculated by using J–O theory, and the intensity parameters Ω_2, Ω_4 and Ω_6 are 14.197×10^{-20} cm^2, 4.303×10^{-20} cm^2 and 6.352×10^{-20} cm^2, respectively. The maximum absorption cross section at 808 nm is 8.7×10^{-20} cm^2 and the FWHM is 6 nm. The strongest emission is located at 1066.3 nm, and the emission cross section is 29×10^{-20} cm^2. The florescence lifetime of $^4F_{3/2}$ is 152 μs. A maximum output power of 1.12 W is obtained with the incident power of 5.0 W, corresponding to an optical-to-optical conversion efficiency of 22.4% and a slope efficiency of 24.0%. All the results suggest that Nd:$YNbO_4$ crystal is a new LD pumped laser material with good performance. In future work, we will improve the technology of crystal growth and optimize the cavity to realize more efficient laser output.

Acknowledgment

This work was financially supported by the National Natural Science Foundation of China (Grants Nos. 61205173, 51272254, 51502292, and 61405206), and the Knowledge Innovation Program of the Chinese Academy of Sciences (Grant No.CXJJ-15M055).

References

[1] H.H. Yu, K. Wu, B. Yao, H.J. Zhang, Z.P. Wang, J.Y. Wang, X.Y. Zhang, M.H. Jiang, Opt. Lett. 35 (2010) 1801.
[2] R.W. Farley, P.D. Dao, Appl. Opt. 34 (1995) 4269.
[3] E. Herault, F. Balembois, P. Georges, Opt. Express 13 (2005) 5653.
[4] H.H. Yu, J.H. Liu, H.J. Zhang, A.A. Kaminskii, Z.P. Wang, J.Y. Wang, Laser Photonics Rev. 8 (2014) 847.
[5] R. Scheps, J. Myers, G. Mizell, Appl. Opt. 33 (1994) 5546.
[6] V. Lupei, N. Pavel, Y. Sato, T. Taira, Opt. Lett. 28 (2003) 2366.
[7] F. Peng, H.J. Yang, Q.L. Zhang, J.Q. Luo, W.P. Liu, D.L. Sun, R.Q. Dou, G.H. Sun, Appl. Phys. B 118 (2015) 549.
[8] R.Q. Dou, Q.L. Zhang, D.L. Sun, J.Q. Luo, H.J. Yang, W.P. Liu, G.H. Sun, Cryst. Eng. Comm. 16 (2014) 11007.
[9] R.Q. Dou, Q.L. Zhang, W.P. Liu, J.Q. Luo, X.F. Wang, S.J. Ding, D.L. Sun, Opt. Mater 48 (2015) 80.
[10] M. Nazarov, Y.J. Kim, E.Y. Lee, K. Min, M.S. Jeong, S.W. Lee, D.Y. Noh, J. Appl. Phys. 107 (2010) 103104.
[11] S.H. Shin, D.Y. Jeon, K.S. Suh, J. Appl. Phys. 90 (2001) 5986.
[12] M. Yang, Q.L. Li, Y. Wang, X.Y. Liu, X.F. Wang, 1050, Chem. Res. Chin. Univ. 29 (2013).
[13] L.H. Brixner, H.Y. Chen, J. Electronchem. Soc. 130 (1983) 2435.
[14] G.M. Wolten, ActaCryst 23 (1967) 939.
[15] A.C. Larson, R.B.V. Dreele, General Structure Analysis System, Los Alamos National Laboratory Report No. LAUR, 2004, p. 86.
[16] G.H. Sun, Q.L. Zhang, H.J. Yang, J.Q. Luo, D.L. Sun, C.J. Gu, S.T. Yin, Master. Chem. Phys. 138 (2013) 162.
[17] W.P. Liu, Q.L. Zhang, W.L. Zhou, C.J. Gu, S.T. Yin, Trans. Nucl. Sci. 57 (2010).
[18] G.S. Ofelt, J. Chem. Phys. 37 (1962) 511.
[19] B.R. Judd, Phys. Rev. 127 (1962) 750.
[20] D.Z. Li, X.D. Xu, D.H. Zhou, S.D. Zhuang, Z.P. Wang, C.T. Xia, F. Wu, J. Xu, Laser Phys. Lett. 7 (2010) 798.
[21] Z. Pan, H.H. Yu, H.J. Cong, H.J. Zhang, J.Y. Wang, Q. Wang, Z.Y. Wei, Z.G. Zhang, R.I. Boughton, Appl. Opt. 51 (2012) 7144.
[22] R. Peterson, H.P. Jenssen, A. Cassanho, Adv. Solid-State Lasers 68 (2002) 294.
[23] B.F. Aull, H.P. Jenssen, IEEE J. Quantum Electron 18 (1982) 925.
[24] S.Q. Sun, H.H. Yu, Y.C. Wang, H.J. Zhang, J.Y. Wang, Opt. Express 21 (2013) 31119.
[25] S.Q. Sun, J. Mater. Res. 27 (2012) 2528.
[26] A.A. Demidovich, A.P. Shkadarevich, M.B. Danailov, P. Apai, T. Gasmi, V.P. Gribkovskii, A.N. Kuzmin, G.I. Ryabtsev, L.E. Batay, Appl. Phys. B 67 (1998) 11.